ORIGINAL PAPER

4D flow vs. 2D cardiac MRI for the evaluation of pulmonary regurgitation and ventricular volume in repaired tetralogy of Fallot: a retrospective case control study

Kimberley G. Jacobs[1,4] · Frandics P. Chan[1] · Joseph Y. Cheng[1] · Shreyas S. Vasanawala[2] · Shiraz A. Maskatia[1,3]

Abstract

Lengthy exams and breath-holding limit the use of pediatric cardiac MRI (CMR). 3D time-resolved flow MRI (4DF) is a free-breathing, single-sequence exam that obtains magnitude (anatomic) and phase contrast (PC) data. We compare the accuracy of gadobenate dimeglumine-enhanced 4DF on a 1.5 T magnet to 2D CMR in children with repaired tetralogy of Fallot (rTOF) to measure pulmonary net flow (PNF) as a reflection of pulmonary regurgitation, forward flow (FF) and ventricular volumetry. Thirty-four consecutive cases were included. 2D PCs were obtained at the valve level. Using 4DF, we measured PNF at the valve and at the main and branch pulmonary arteries. PNF measured at the valve by 4DF demonstrated the strongest correlation ($r = 0.87$, $p < 0.001$) and lowest mean difference (3.5 ± 9.4 mL/beat) to aortic net flow (ANF). Semilunar FF and stroke volume of the respective ventricle demonstrated moderate-strong correlation by 4DF ($r = 0.66$–0.81, $p < 0.001$) and strong correlation by 2D ($r = 0.81$–0.84, $p < 0.001$) with similar correlations and mean differences between techniques ($p > 0.05$). Ventricular volumes correlated strongly between 2D and 4DF ($r = 0.75$–0.96, $p < 0.001$), though 4DF overestimated right ventricle volumes by 11.8–19.2 mL/beat. Inter-rater reliability was excellent for 2D and 4DF volumetry ($ICC = 0.91$–0.99). Ejection fraction moderately correlated ($r = 0.60$–0.75, $p < 0.001$) with better reliability by 4DF (ICC: 0.80–0.85) than 2D (ICC: 0.69–0.89). 4DF exams were shorter than 2D (9 vs. 71 min, $p < 0.001$). 4DF provides highly reproducible and accurate measurements of flow with slight overestimation of RV volumes compared to 2D in pediatric rTOF. 4DF offers important advantages in this population with long-term monitoring needs.

Keywords 4D flow MRI · Cardiac MRI · Tetralogy of fallot · Congenital heart disease

---

Shreyas S. Vasanawala and Shiraz A. Maskatia have contributed equally to this work.

✉ Kimberley G. Jacobs
   kjacobs9@stanford.edu

1   Department of Pediatrics, Stanford University School of Medicine, Palo Alto, CA, USA

2   Divisions of Pediatric Radiology and Cardiovascular Imaging, Department of Radiology, Stanford University School of Medicine, Palo Alto, CA, USA

3   Divisions of Pediatric Cardiology and Cardiovascular Imaging, Department of Pediatrics, Stanford University School of Medicine, Palo Alto, CA, USA

4   Lucile Packard Children's Hospital, 725 Welch Rd, Room G71, MC 5906, Palo Alto, CA 94304, USA

Abbreviations

4DF	3D time-resolved flow
ANF	Aortic net flow
BPA	Branch pulmonary arteries
CMR	Cardiac magnetic resonance imaging
EDV	End diastolic volume
EDVi	End-diastolic volume index
EF	Ejection fraction
ESV	End systolic volume
ESVi	End-systolic volume index
FF	Forward flow
IQR	Interquartile range
LOA	Limits of agreement
LV	Left ventricle
MAPCA	Major aortopulmonary collateral arteries
MPA	Main pulmonary artery
PC	Phase contrast
PNF	Pulmonary net flow
PR	Pulmonary regurgitation

PV   Pulmonary valve
PVR   Pulmonary valve replacement
RV   Right ventricle
rTOF   Repaired tetralogy of Fallot
SD   Standard deviation
SSFP   Steady state free precession
SV   Stroke volume
VENC   Velocity encoded

Introduction

Estimated prevalence of tetralogy of Fallot is 3.97/10,000 births in the US, or approximately 1700 new cases per year [1]. After initial repair, many of these patients develop symptoms of chronic right ventricular overload and are at high risk for biventricular dysfunction leading to heart failure, arrhythmias, and sudden death [2–4]. This morbidity and mortality is in part due to pulmonary regurgitation (PR) [2], which has led to multiple studies investigating the ideal timing of pulmonary valve replacement (PVR) based on the degree of PR and ventricular dilation to optimize post-surgical outcomes [5–8]. Thus, long-term management, particularly the timing of interventions, relies on accurate measurement of pulmonary regurgitation, ventricular volumes, and ventricular function.

Cardiac MRI (CMR) is the gold standard for these measurements in repaired tetralogy of Fallot (rTOF) patients [9]. Longitudinal follow-up with CMR for pediatric patients is recommended every 3 years in stable patients and up to yearly in patients with known moderate RV dilation, interim worsening RV dilation, or evidence of RV dysfunction, similar to recommendations for adults [10, 11]. However, traditional 2D CMR has several limitations including prolonged breath holding, immobility during scan, and lengthy scan times of 1–2 h commonly requiring sedation in patients younger than 6–8 years of age and/or those with developmental delay [9]. Each exam requires a highly trained CMR technologist familiar with pediatric congenital heart disease and oversight from a cardiologist or radiologist to determine scan planes and acquisition parameters [12].

3D time-resolved flow (4DF) MRI is a 5–10 min, free-breathing, single acquisition imaging sequence that simultaneously acquires magnitude and phase contrast data without a pre-study protocol. This allows for anatomic, volumetric, and flow information to be obtained from this single sequence. Prior work has demonstrated accuracy and reliability in measurements of flow as well as ventricular volumes, function, and mass comparable to or better than 2D CMR [13–21]. However, these studies included a heterogeneous patient population, use of a 3-T magnet, or use of uncommon or now unavailable contrast agents, thereby limiting generalizability. A small focused study of rTOF

patients showed feasibility of 4DF to measure net flow, peak velocity, and visualize vortices, but did not determine accuracy of flow measurements compared to a reference standard, such as 2D CMR [22]. Other work with 4DF in rTOF patients are focused primarily on flow patterns and energetics [23–26].

At our institution, use of 4DF CMR on the 1.5-T magnet with commonly available contrast agents such as gadobenate dimeglumine has become standard practice as the final acquisition after a comprehensive 2D CMR exam, but accuracy of 4DF CMR measurements with this magnet and contrast have not been studied. In pediatric patients with rTOF, our objectives were: to assess the accuracy of 4DF CMR to measure pulmonary net flow (PNF) as a reflection of PR, to compare ventricular stroke volume to forward flow, and to compare volumetry measurements obtained by 4DF CMR to those obtained by the clinical standard, 2D CMR.

Material and methods

Study population

We retrospectively identified consecutive patients with rTOF referred for CMR at Lucile Packard Children's Hospital from 10/2014–2/2018. We included patients with TOF and pulmonary atresia who had undergone an RV to PA conduit and ventricular septal defect closure and patients with double outlet RV and normally related great arteries and pulmonary or sub-pulmonary stenosis who were thought to be physiologically similar to patients with TOF at the time of initial repair. Patients with pulmonary atresia and major aortopulmonary collateral arteries (MAPCAs) were included if fully unifocalized to an RV to PA conduit. We excluded patients with residual shunt lesions, those who underwent CMR studies on a 3 T system, and those who received contrast agents other than gadobenate dimeglumine (Multihance, Bracco Diagnostics, Monroe, NJ). The Stanford University IRB approved this study and waived informed consent.

Image acquisition

All studies were performed on a 1.5-T system (GE Healthcare, OPTIMA 450W). Data for 2D CMR volumetric analyses were obtained using short-axis balanced steady state free precession (bSSFP) acquisitions. Short-axis sequences were obtained with a breath hold using one signal average, and included 12–14, 8–10 mm slices spanning the ventricles, minimum matrix 160×192, flip angle 50°, with retrospective gating to generate 20 phases per cardiac cycle as is our institutional standard [9]. 2D PC imaging was performed at the level of the aortic valve (AoV) and pulmonary valve (PV), with scan parameters including 2–3

signal average free-breathing, 10 mm slice thickness, minimum matrix 160×192, velocity encoded range (VENC) of 150–350 cm/s, and 20–25 phases per cardiac cycle. No corrections were employed during post-processing, as no baseline error was noted.

4DF acquisitions were obtained at the end of each CMR study following administration of 0.15 mmol/kg (0.3 ml/kg) of gadobenate dimeglumine. Gadobenate offers the benefits of higher T1 relaxivity and longer half-life with resultant improved signal to noise ratio for the duration of the study. As improved gradient systems have allowed for shorter TRs and higher frequencies of excitations resulting in signal loss, use of contrast for enhancement of 4DF sequences has become standard practice at our institution [12].

Each study included performance of an MR angiogram prior to acquisition of the 4DF sequence. 4DF scan parameters included a flip angle of 15°, resolution of $0.8 \times 0.8 \times 1.4$ mm³, acquired matrix $224 \times 192 \times 76$, minimum TE of 1.8–2.1 ms, minimum repetition time (TR) of 3.9–4.3 ms with an additional 5.1 ms for fat-saturation, retrospective gating creating 20 phases per cardiac cycle, temporal resolution of 68 ms (range 45–73), sampling reduction factor of 2.4×4.4 before k-space corner cutting, views-per-segment of 2–6 depending on heart rate, bandwidth of ± 83.33 kHz, and velocity encoding range (VENC) of 250 cm/s. The field of view spanned from above the aortic arch to the diaphragm and laterally to the first order branching of the pulmonary arteries. To minimize coherent artifacts from respiratory motion, a pseudo-random view-ordering and sampling was used for 4DF [27]. More specifically, a variable-density Poisson disc sampling mask was first generated. Each (ky, kz)-sample was then grouped into radial spokes and ordered according to the golden-ratio [28]. Post-processing using cloud-based software (Arterys, San Francisco, CA) adjusted for phase correction by performing a polynomial fit to the phase errors estimated from the static tissue.

Image analysis and comparisons

Subjects were analyzed in a blinded fashion, with at least 10 studies separating corresponding 2D and 4DF CMR images. KGJ, a pediatrics resident, collected all measurements in this study after receiving 12 h of one-on-one instruction and feedback by a cardiologist with expertise in CMR (SAM) on studies from similar patients not included in this study. The senior author (SAM) qualitatively reviewed ~ 20% of the measurements to verify contour selection periodically during the data analysis period and obtained inter-observer reliability data on a separate 10 subjects selected through a random number generator.

2D PC images were analyzed on QFlowMR (MEDIS; Leiden, NL). A region of interest was traced around the AoV and PV with the velocity therein integrated to determine the flow volume [29]. Pulmonary flow by 2D CMR was measured only at the PV level, as our institutional practice. 4DF visualization and flow analyses were performed using Arterys. Pulmonary flow was measured at three locations: PV, main pulmonary artery (MPA, determined as the most distal portion of the pulmonary trunk proximal to bifurcation), and branch pulmonary arteries (BPAs, the sum of the respective left and right pulmonary arteries obtained just distal to bifurcation) (Fig. 1). Cross-sectional planes were angulated orthogonal to the direction of flow and vessel anatomy, and a region of interest was traced, similar to 2D PC methodology. Valve tracking was not employed and through plane motion was not accounted for on either 2D or 4DF CMR analyses.

2D volumetric images were analyzed on QMassMR (MEDIS; Leiden, NL). A series of short-axis images were manually traced along endocardial borders to calculate end-diastolic volumes (EDV) and end-systolic volumes (ESV) for the right ventricle (RV) and left ventricle (LV), respectively. The 2- and 4-chamber views were used to cross-reference contours [30]. A slice was considered to contain primarily

Fig. 1 4DF CMR streamline visualization of the left ventricular outflow tract (left image) and right ventricular outflow tract (right image). Cross-sectional analysis planes were manually positioned at the aortic valve (**a**), pulmonary valve (**b**), main pulmonary artery (**c**), and branch pulmonary arteries (**d**)
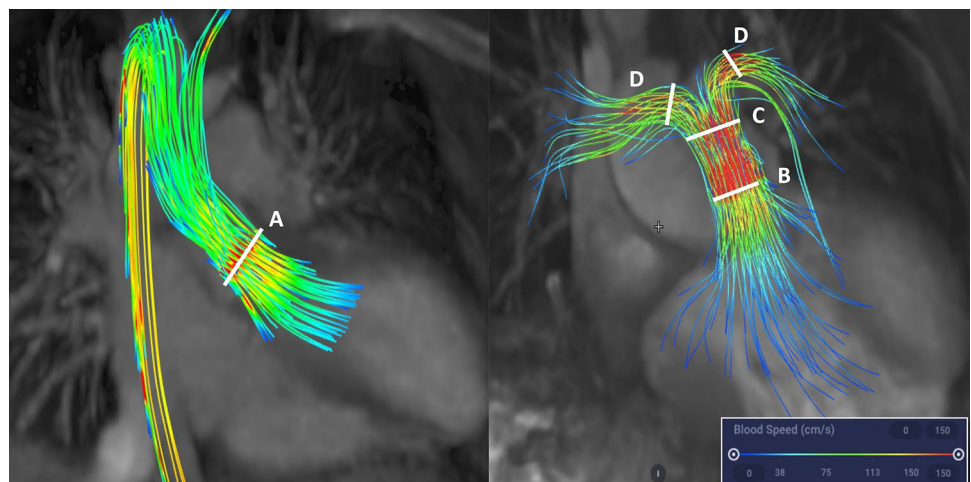
atrium when < 50% of the blood volume was encircled with myocardium, outflow tracts were included in ventricular volumes up to the semilunar valve cusps, and trabeculations and papillary muscles were considered part of the blood pool [31]. For 4DF volumetry, anatomic landmarks (mitral valve, tricuspid valve, AoV, PV, and LV and RV apices) were identified to create two- and four-chamber views using artificial intelligence (Supp Fig. 1). A series of 12 short-axis slices were generated spanning the ventricles. Each slice was similarly manually traced for endocardial borders without the use of semi-automated interpolated tracing.

Multiple comparisons were made in this study. Our primary objective was to measure pulmonary net flow as a surrogate for pulmonary regurgitation. Pulmonary net flow, calculated as pulmonary forward flow (FF) minus regurgitant flow, was compared to aortic net flow (ANF) of the same patient as a reference standard for stroke volume (SV). With perfect accuracy, there would be no difference between PNF and ANF since all patients were without shunt lesions. We compared 2D ANF to 2D PNF measured at the PV, and 4DF ANF to PNF measured at the PV, MPA, and BPAs, respectively. Accuracy of semilunar FF was compared to SV of the respective ventricle by volumetry as a measure of internal consistency. Of note, patients with tricuspid regurgitation ≥ 5% (n = 3, range 10–21%) as measured by CMR were excluded from the analyses comparing RV SV to pulmonary FF. Tricuspid regurgitation was calculated by directly measuring the regurgitant jet by 4DF as per our institutional standard practice [32]. To further study utility of 4DF CMR, we directly compared PNF and PR measurements by 4DF and 2D CMR given their clinical importance in the rTOF population. PR was calculated as ((pulmonary FF-PNF)/PNF)*100 and considered mild if < 20%, moderate if 20–40%, and severe if > 40% [33].

Our secondary objective was to assess accuracy of 4DF CMR to measure ventricular size and function compared to 2D CMR. Volumes were indexed to body surface area, calculated using the Haycock formula [34]. Stroke volume (SV) was calculated as EDV-ESV for each respective ventricle. Ejection fraction (EF) was calculated as ((EDV-ESV)/EDV) × 100.

Statistical analysis

Continuous variables were described as mean ± standard deviation (SD) and median [interquartile range (IQR)] as appropriate based on assessments of normality with Shapiro–Wilk tests and histograms. Correlations between methods were assessed using Pearson (r) or Spearman (ρ) correlation coefficients, as appropriate, and interpreted as follows: 0.3–0.5 weak, 0.5–0.7 moderate, and > 0.7 strong. Pearson correlation coefficients were compared using a Fisher's r to z transformation. Differences between methods were compared using the paired T-test and Wilcoxon signed rank test, as appropriate. The presence of any systematic bias was represented by both the mean difference and absolute mean difference as these represent two types of variance. For example, in cases of equal variance around zero, the mean difference is small while the absolute mean difference represents a better distribution of measurement variance. Differences were calculated as ANF minus PNF, SV minus FF, and 2D minus 4DF volumetry measurements. Agreement was assessed via Bland–Altman analysis, plotted as the difference between measurements against the measurement mean with variance represented by the span of the limits of agreement (LOA = mean difference ± 1.96 × SD of differences) as previously described [35]. Inter-rater reliability was assessed with intra-class correlation coefficients (ICC) using a two-way mixed model with absolute agreement. $p < 0.05$ was considered statistically significant. All statistical analyses were performed using statistical software (IBM SPSS Statistics for Macintosh, Version 25.0. Armonk, NY: IBM Corp).

Results

Thirty-seven patients met inclusion criteria during the study time period. Three (8%) were excluded due to excessive aliasing on 4DF ($n = 2$) and insufficient 2D image quality ($n = 1$), resulting in a study cohort of thirty-four patients (Table 1). Heart rates were similar between methods (2D 72.6 ± 13.7 beats/min, 4DF 72.4 ± 13.6 beats/min, p = 0.84). Average time to complete 2D CMR acquisitions was 71.2 ± 18.8 vs. 9.2 ± 1.3 min for 4DF acquisitions

Table 1 Patient demographics (n = 34)

Age (years)	15.6 ± 3.6
Sex (F)[a]	58.8% (n = 20)
Height (cm)	154.1 ± 18.9
Weight (kg)	54 ± 14.5
BSA (m²)	1.47 ± 0.3
Congenital heart disease	
Tetralogy of Fallot	91.2% (n = 31)
PA/VSD	5.9% (n = 2)
Double outlet right ventricle	2.9% (n = 1)
Additional cardiac defects	
Bicuspid pulmonary valve	2.9% (n = 1)
Right aortic arch	5.9% (n = 2)
MAPCAs	8.8% (n = 3)
Syndromes	
DiGeorge syndrome	5.9% (n = 2)

BSA body surface area, *cm* centimeters, *kg* kilograms, *m* meters, *MAPCAs* major aortopulmonary collateral arteries, *PA/VSD* pulmonary atresia/ventricular septal defect

(p < 0.001), consistent with prior work on the length of 4DF CMR [12–14, 16].

Assessment of PNF

PNF was underestimated relative to ANF by small, but statistically significant, differences (5.4–11.7% of mean flow, p < 0.04) across all three 4DF CMR comparisons and trended towards a significant difference for 2D CMR (9% of mean flow, p = 0.055) (Table 2) (Fig. 2). These mean differences were overall similar between methods (p > 0.35). PNF and ANF correlated stronger by 4DF (PV, MPA, BPA: r = 0.77–0.87, p < 0.001) than 2D CMR (r = 0.68, p < 0.001) (Table 2). Specifically, measurement of PNF at the level of the PV by 4DF CMR demonstrated the strongest correlation with ANF (r = 0.87, p < 0.001) and lowest mean difference (3.5 ± 9.4 mL/beat). Measurements of ANF and PNF at the PV had higher variance by 2D CMR than 4DF CMR; LOA for 2D CMR were − 33 mL/beat (− 41.8% of mean) to 47 mL/beat (59.6% of mean) compared to LOA for 4DF CMR of − 16 mL/beat (− 23% of mean) to 24 mL/beat (34% of mean). Similarly, the absolute mean difference between ANF and PNF evaluated at the PV was significantly larger using 2D CMR than 4DF (p < 0.001).

PNF showed good agreement between 2D and 4DF CMR (mean difference 5.4 ± 19.0 mL/beat, p = 0.11) and correlated moderately (r = 0.67, p < 0.001). Inter-rater reliability of PNF was excellent for 2D (ICC = 0.80) and 4DF CMR (ICC = 0.87) (Table 5). The degree of PR ranged from mild to moderate with good agreement between methods (median (IQR): 2D PC 23.4% (5.4–40.8%); 4DF 25.8% (10.5–36.6%); p = 0.23) and a strong correlation (ρ = 0.78, p < 0.001).

Assessment of FF

Pulmonary FF was accurate compared to RV SV with small mean differences for all 4DF CMR (1.0–5.9% of mean volume, p > 0.18) and 2D CMR measurements (1.3% of mean volume, p = 0.71) (Table 3) (Fig. 3). Though correlations between pulmonary FF and RV SV were slightly stronger with 2D (r = 0.81, p < 0.001) than 4DF CMR (r = 0.66–0.71, p < 0.001), this trend was not significant (2D PV vs. 4DF PV, p = 0.11; 2D PV vs. 4DF MPA, p = 0.13; 2D PV vs. 4DF BPA, p = 0.18). There was good agreement between methods for mean differences (p = 0.11) and absolute mean differences (p = 0.20). LOA were overall similar between 4DF and 2D CMR measurements.

Aortic FF was accurate compared to LV SV by 4DF CMR (4.7% of mean volume, p = 0.15) and correlated strongly (r = 0.81, p < 0.001) but was significantly different to LV SV by 2D CMR (9.4% of mean volume, p = 0.01) despite similarly strong correlations. LV SV to aortic FF showed good agreement between methods with similar mean differences (p = 0.24), absolute mean differences (p = 0.11), and Pearson correlation coefficients (p = 0.32). LOA were narrower for 4DF than 2D CMR measurements (Fig. 3).

Assessment of ventricular indices

Ventricular indices were moderately-strongly correlated for LV (EF r = 0.60, volumes r = 0.75–0.87, all p < 0.001) and strongly correlated for RV (EF r = 0.75, volumes r = 0.95–0.96, all p < 0.001) between methods (Table 4) (Fig. 4). Despite strong correlations, 4DF CMR overestimated RV volumes (RVEDVi 11.8 mL/beat, 7.5% of mean volume; RVESVi 19.2 mL/beat, 20.8% of mean volume; p < 0.001 respectively) and function (8% EF, 18.8%

Table 2 Comparison of aortic and pulmonary net flow (n = 34)

	ANF	PNF	Pearson (r)	Paired T-test (p value)	Mean difference (± SD)	Absolute mean difference (± SD)
2D ANF vs. PV NF	81.8 ± 26.1	74.6 ± 24.2	0.68	0.06	7.0 ± 20.3[a]	14.2 ± 15.9[b]
4DF ANF vs. PV NF	72.6 ± 16.8	69.1 ± 19.1	0.87	0.04*	3.5 ± 9.4[a]	7.2 ± 8.2[b]
4DF ANF vs. MPA NF		64.7 ± 19.2	0.77	< 0.01*	8.0 ± 12.2[a]	10.5 ± 10.0
4DF ANF vs. BPA NF		65.5 ± 14.6	0.80	< 0.01*	7.3 ± 9.9[a]	9.2 ± 8.1

Mean difference/absolute mean difference calculated as ANF – PNF, units = mL/beat. All Pearson correlation coefficients are significant, p < 0.001

ANF Aortic net flow, *BPA* branch pulmonary arteries, *MPA* main pulmonary artery, *NF* net flow, *PNF* pulmonary net flow, *PV* pulmonary valve, *SD* standard deviation

*Denotes statistical significance (p < 0.05)

[a]No difference in mean differences between 2D and respective 4D methods (p > 0.35)

[b]There was a significantly larger absolute mean difference between ANF and PNF with 2D versus 4DF at the PV (p < 0.01)
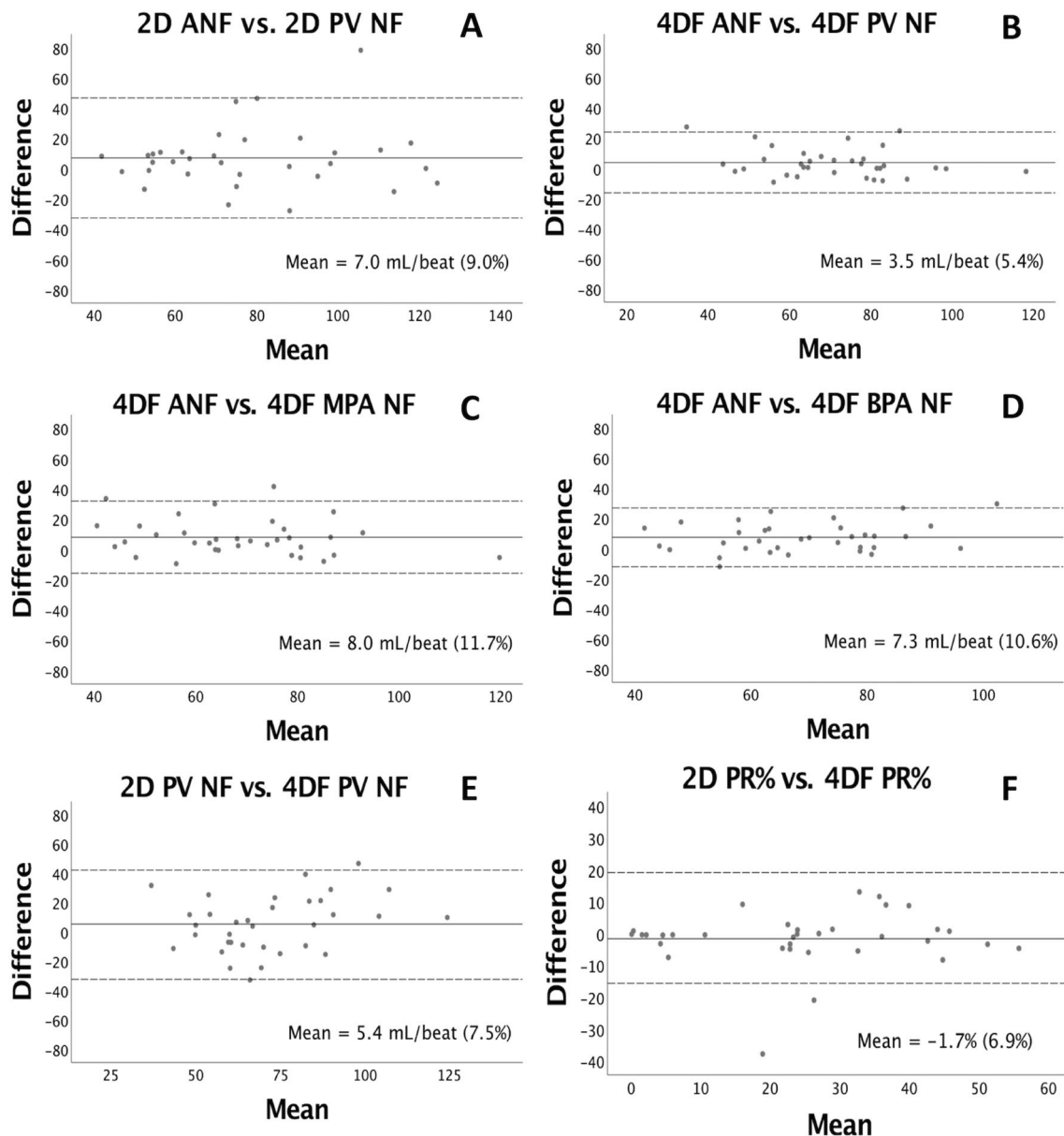
Fig. 2 Bland Altman plots comparing ANF and PNF by 2D CMR (**a**) and 4DF CMR (**b–d**, measured at the PV, MPA, and BPA, respectively); differences are calculated as ANF–PNF. **e**, **f** directly compare PNF and PR% measured at the PV between 2D and 4DF CMR. Units = mL/beat (**a–e**) and % regurgitation (**f**). The mean difference, represented as the solid line, is reported as X (% of mean volume or regurgitation). The limits of agreement are represented with dashed lines. *ANF* aortic net flow, *BPA* branch pulmonary arteries, *MPA* mean pulmonary arteries, *PNF* pulmonary net flow, *PR* pulmonary regurgitation, *PV* pulmonary valve

of mean function, p < 0.001). Conversely, LV measurements were overall similar between techniques (LVEDVi p < 0.01, LVESVi p = 0.33, LVEF p = 0.38). Inter-rater reliability was excellent for RV (ICC 0.98–0.99) and LV volumetry (ICC 0.91–98) for both methods, and reliability for RV and LV EF was better for 4DF than 2D (Table 5). Inter-rater measurement variance, reported as mean difference (LOA), was similar for 2D and 4DF volumetry (p > 0.3).

Discussion

In this study, we assessed the accuracy of 4DF CMR to measure PNF relative to ANF and to measure pulmonary FF relative to RV stroke volume. We also assessed the accuracy of ventricular volumetry measured on 4DF sequences relative to standard 2D CMR sequences. We found that gadobenate dimeglumine-enhanced 4DF

Table 3 Comparison of stroke volume and forward flow within systemic (n = 34) and pulmonary (n = 31) circulations

TABLE 3	SV	FF	Pearson (r)	Paired T-test (p value)	Mean difference (± SD)	Absolute mean difference (± SD)
2D LVSV vs. Ao FF	76.1 ± 19.9	83.4 ± 27.0	0.84	0.01*	− 7.4 ± 14.2	12.5 ± 10.1
4D LVSV vs. Ao FF	70.3 ± 20.1	73.5 ± 17.3	0.81	0.15	− 3.3 ± 11.8[b]	9.3 ± 7.8[b]
2D RVSV vs. PV FF	101.5 ± 28.8	100.3 ± 31.9	0.81	0.71	1.3 ± 18.7	13.5 ± 12.8
4D RVSV vs. PV FF	89.7 ± 25.1	95.2 ± 27.2	0.66	0.18	− 5.5 ± 21.5[c]	17.3 ± 13.5[c]
4D RVSV vs. MPA FF		90.6 ± 25.3	0.68	0.80	− 0.9 ± 20.3[c]	15.7 ± 12.7[c]
4D RVSV vs. BPA FF		86.0 ± 18.6	0.71	0.253	3.7 ± 17.8[c]	14.3 ± 10.9[c]

Subjects with > 5% tricuspid regurgitation (n = 3) excluded from RVSV vs. pulmonary FF analyses. Mean difference/absolute mean difference calculated as SV–FF, units = mL/beat

Ao aorta, *BPA* branch pulmonary arteries, *FF* forward flow, *LVSV* left ventricular stroke volume, *MPA* main pulmonary artery, *PV* pulmonary valve, *RVSV* right ventricular stroke volume, *SD* standard deviation

[a]Denotes statistical significance (p < 0.05)

[b]No significant difference compared to 2D LVSV vs Ao FF (p > 0.31)

[c]No significant difference compared to 2D RVSV vs PV FF (p > 0.14)

sequences acquired on a 1.5-T system demonstrated superior accuracy to 2D PC for measurements of flow and were comparable to 2D SSFP for accuracy of volumetry. Assessment of PNF was the most accurate by 4DF CMR at the level of the PV, with the strongest correlation (r = 0.87, p < 0.001), the smallest mean difference (3.5 ± 9.4 mL/beat), and lowest variance (LOA: − 16 to 24 mL/beat; − 23% to 34%) relative to ANF. FF was accurate by 4DF CMR with moderate-strong correlations and small mean differences compared to the respective ventricle's SV. PR showed good agreement when measured at the PV with strong correlation ($\rho = 0.78$, p < 0.001) and a clinically acceptable median (IQR) difference between 2D and 4DF CMR of 0.5% (− 4.7 to 1.1%), p = 0.23. Measurements of RV volumetry by 4DF strongly correlated (r = 0.95–0.96, p < 0.001) with 2D SSFP but were overestimated by ~ 7.5% of mean volume for RVEDVi and ~ 20% of mean volume for RVESVi. This is likely a true overestimation as absolute agreements between raters for 2D SSFP and 4DF volumetry were excellent (ICC = 0.98–0.99) with small mean differences (0.5–5.4 mL/m^2). Despite a strong correlation, 4DF CMR also overestimated RV function by ~ 8% on average. On average, complete 2D studies took over one hour longer than 4DF acquisitions.

Our study is the first to compare 4DF CMR obtained on a 1.5 T gradient system with gadobenate dimeglumine contrast to standard 2D CMR in the comprehensive hemodynamic assessment of patients with rTOF. Several works have previously shown that 4DF measurements have good agreement to 2D CMR data using gadofosveset on the 1.5 T MRI, which is likely due to gadofosveset's improved signal to noise ratio and hence improved image quality [14, 19]. Similarly, a study using ferumoxytol and 3 T MRI reported strong correlations in ventricular volumetry, function and mass between 2D and 4DF CMR [16]. However, these contrast agents are not in standard use as gadofosveset (Ablavar, Lantheus Medical Imaging, MA) was discontinued in 2017 and ferumoxytol (Feraheme; AMAG Pharmaceuticals, Waltham, MA), while used clinically at an increasing number of centers for cardiac imaging, carries a black box warning in pediatric imaging due to the small risk of adverse reactions [36, 37]. Further, the majority of pediatric cardiac imaging is completed using a 1.5 T MRI. Use of a gadolinium-based contrast agent and a 1.5-T system reflects resources found in a typical clinical setting and increases generalizability of the results presented in this study. To emphasize the effects stronger gradient systems and higher signal to noise ratio contrast agents can have on image quality, a typical 2D SSFP short axis image using a 1.5-T system, short axis view derived from ferumoxytol-enhanced 4DF acquisitions obtained using a 3-T system, and a short axis view derived from gadobenate dimeglumine-enhanced 4DF acquisition using a 1.5-T system are provided in the appendix (Supp Fig. 2).

The primary objective of this study was to assess the accuracy of 4DF CMR to measure PNF as a surrogate for PR. Our approach differs from prior works that directly compared measurements by 2D and 4DF CMR [13, 19-21, 38,
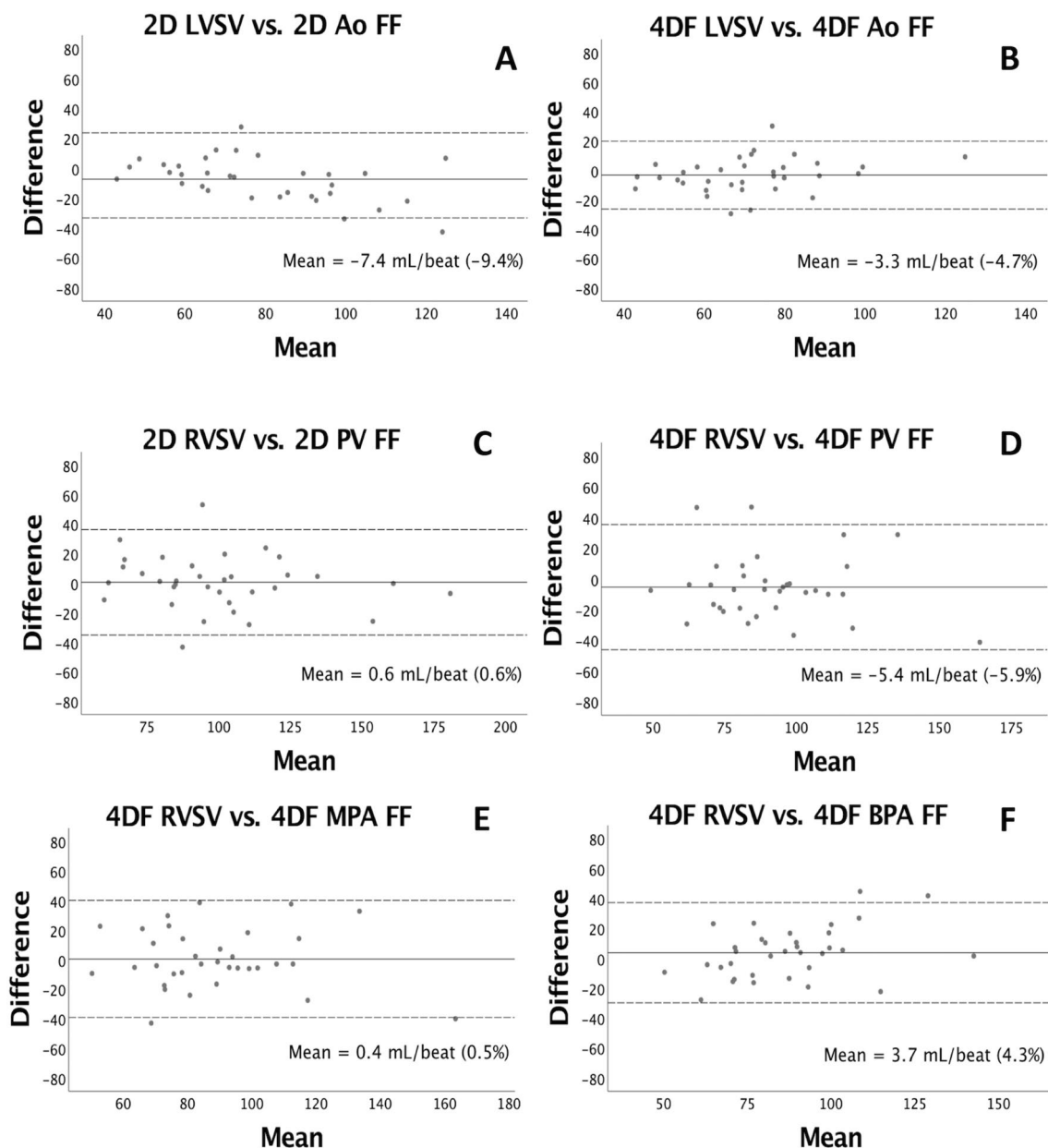
Fig. 3 Bland Altman Plots comparing SV and FF for the systemic circulation (**a**, **b**) and pulmonary circulation (**c–f**). Differences are calculated as SV–FF. The mean difference, represented as the solid line, is reported as X (% of mean flow). The limits of agreement are represented with dashed lines. *Ao* aorta, *BPA* branch pulmonary arteries, *FF* forward flow, *LV* left ventricle, *MPA* main pulmonary artery, *PV* pulmonary valve, *RV* right ventricle, *SV* stroke volume

39] as this study takes advantage of the internal consistency within CMR by using reference standards measured by the study (PNF to ANF, FF to SV). Our measurements of PNF were accurate compared to ANF, with differences around 10% of mean flow which is considered clinically acceptable [19]. As all patients had PR and no intracardiac shunt, the variation between ANF and PNF reflects error in measurement of pulmonary regurgitant flow. Patients with rTOF may have a combination of pulmonary stenosis and regurgitation, which can lead to turbulent flow, dephasing within a volume,

and resultant signal loss with PC MRI [39-41]. Prior works have also demonstrated that placement of cross-sectional planes at the peak flow velocity [39] and use of retrospective valve-tracking [42, 43] can further increase accuracy of flow measurements.

The second objective of our study was to compare the accuracy of volumetry measurements of 4DF compared to 2D CMR. Several studies have previously compared these methods. On a 1.5-T magnet with a combination of gadobenate and gadofosveset, LOA of − 42% to 38% of mean

Table 4 Comparison of ventricular volume and function measurements via 2D SSFP and 4DF (n = 34)

	2D	4DF	Pearson (r)	Paired T-test (p value)	Mean difference (± SD)
LVEDVi (mL/m^2)	93.7 ± 20.4	88.2 ± 21.0	0.87	< 0.01	5.4 ± 10.6
LVESVi (mL/m^2)	42.4 ± 10.8	40.7 ± 13.4	0.75	0.33*	1.5 ± 8.8
LV SV (mL/m^2)	51.5 ± 11.8	47.5 ± 10.8	0.89	< 0.01	4.0 ± 5.4
LV EF (%)	55.1 ± 5.0	54.3 ± 6.3	0.60	0.38*	0.8 ± 5.2
RVEDVi (mL/m^2)	152.2 ± 42.5	164.1 ± 48.0	0.96	< 0.01	− 11.8 ± 13.4
RVESVi (mL/m^2)	82.2 ± 27.1	101.4 ± 32.4	0.95	< 0.01	− 19.2 ± 10.7
RV SV (mL/m^2)	62.7 ± 21.8	62.7 ± 21.8	0.89	< 0.01	7.4 ± 9.9
RV EF (%)	46.6 ± 7.6	38.6 ± 7.4	0.75	< 0.01	8.0 ± 5.4

Mean difference = 2D–4DF

LV left ventricle, *RV* right ventricle, *EDV* end-diastolic volume, *ESV* end-systolic volume, *SV* stroke volume, *EF* ejection fraction

*Mean values of LVEF and LVESV were not different between methods (p = 0.33–0.38), but all other mean values were significantly different between 2D and 4DF (p < 0.01)
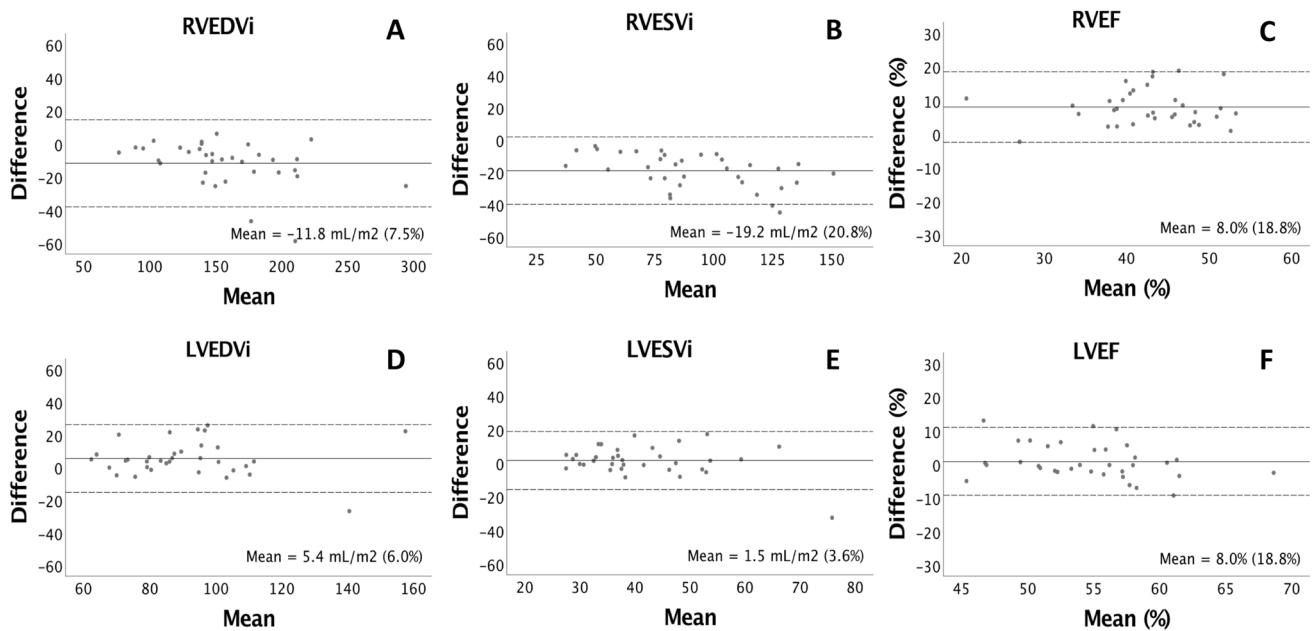

Fig. 4 Bland Altman Plots comparing 2D and 4DF volumetry. The mean difference (2D–4DF), represented as the solid line, is reported as X (% of mean volume or ejection fraction). A one-tailed t-test of the mean difference indicates a significant evidence of bias for all (p < 0.01), except for LVESVi and LVEF (p = 0.33–0.37). The limits of agreement are represented with dashed lines. *EDVi* end-diastolic volume indexed, *EF* ejection fraction, *ESVi* end-systolic volume indexed, *LV* left ventricle, *RV* right ventricle

RV and LV volume were reported [14]. On a 3-T magnet with ferumoxytol, LOA for RVEDV and RVESV similar to ours were reported despite better accuracy of their 4DF volumetry data relative to 2D CMR [16]. The scan-rescan methodology in our study may have affected our comparisons, and several prior works on 2D CMR have attempted to quantify this measurement error. Mooij et al. showed inter-observer repeatability coefficients of RVEDVi 24.1 mL/beat, RVESVi 17.9 mL/beat, and RVEFi 10.7% [44]. In another study, experienced non-blinded radiologists reported intra-observer reliability coefficients of 13.4 mL/beat, 10.1 mL/

beat, and 5.6% respectively [45]. In that study, the radiologists compared contours between studies which may have affected their results to increase precision. This was intentionally avoided in our methodology to minimize observer bias. In comparison to these works, the variability reported between our 2D and 4DF CMR volumetry measurements are similar to previously reported data. Measurement variance was constant irrespective of mean volume, and by extension the size of the patient, which echoes the findings of other 2D and 4DF CMR studies [14, 16, 45]. This suggests that 4DF may be more robust in larger patients which can

Table 5 Inter-rater reliability (n = 10)

	2D		4DF	
	ICC	Mean difference (LOA)	ICC	Mean difference (LOA)
RVEDVi (mL/m^2)	0.98	4.2 (− 21.9, 30.3)	0.98	5.4 (− 9.9, 20.7)
RVESVi (mL/m^2)	0.98	− 0.5 (− 15.2, 14.2)	0.99	1.0 (− 8.6, 10.6)
RVEF (%)	0.89	− 1.4 (− 7.5, 4.7)	0.80	1.8 (− 6.0, 9.6)
LVEDVi (mL/m^2)	0.98	− 3.3 (− 12.9, 6.3)	0.95	− 1.3 (22.4, 19.9)
LVESVi (mL/m^2)	0.91	− 6.6 (− 18.7, 5.6)	0.91	− 2.9 (− 21.7, 15.9)
LVEF (%)	0.69	5.8 (− 3.0, 14.6)	0.85	2.0 (− 4.1, 8.1)
ANF (mL/beat)	0.94	− 2.6 (− 16.7, 11.5)	0.66	1.6 (− 20.4, 23.6)
PNF (mL/beat)	0.80	− 5.3 (− 31.2, 20.6)	0.87	1.6 (− 14.9, 18.1)
PV FF (mL/beat)	0.71	− 1.4 (− 38.2, 35.4)	0.76	7.6 (− 23.2, 38.4)

Intra-class coefficient (ICC) p < 0.001. There are no statistically significant differences between 2D and 4DF mean differences (p > 0.05)

ANF aortic net flow, *EDVi* end-diastolic volume index, *EF* ejection fraction, *ESVi* end-systolic volume index, *LV* left ventricle, *PNF* pulmonary net flow, *PV FF* pulmonary valve forward flow, *RV* right ventricle

be potentially explained by the improved spatial resolution relative to the larger area measured.

4DF has particular advantages in streamlining image acquisition and analysis with a single and short sequence exam. Post-processing on a 4DF dataset allows for selection of an infinite number of orthogonal planes through vasculature. In contrast, 2D CMR requires separate sequences during image acquisition which may require repetition to optimize the plane, further lengthening 2D CMR scans. Susceptibility artifacts from stents or prosthetic valves with metallic rings can be identified and avoided when measuring flow using 4DF post-processing systems. As part of the Arterys artificial intelligence software, two- and four-chamber views are generated after identification of several landmarks. A stack of short-axis volumetric slices is subsequently created, in contrast to 2D CMR acquisitions which require multiple sequences and additional scan time to create the short-axis stack. In our study, 4DF acquisitions took on average less than 10 min, potentially saving over an hour of time relative to traditional 2D CMR. This is of utmost importance in the pediatric population where sedation is required for lengthy studies and is noted to be a significant limitation to CMR.

Based on the findings of this study, we conclude that there is an important role for 4DF imaging in the clinical assessment of patients with rTOF. We found the most accurate measurement of PNF was using 4DF at the PV and therefore recommend 4DF acquisitions over 2D PC acquisitions for assessment of PR when a contrast-enhanced MR angiogram is already being performed. It is enticing to use a single 4DF acquisition as a stand-alone sequence for interval assessment of all patients with rTOF. In our study, ventricular volumes—particularly for the RV—were strongly correlated but did show systematic overestimation using 4DF. It was our impression that 4DF sequences obtained in this study

had lower image quality compared to 2D CMR sequences. As a result, more myocardium may have been included in endocardial tracings, particularly for the RV as the thick myocardium of the LV is easier to identify. The modest correlation between EF measured on 4DF and 2D CMR is likely due to propagated error from EDV and ESV measurements. Inter-observer agreement was excellent for 4DF volumetry, demonstrating that serial measurements using 4DF are sufficiently reliable. However, as reduced ventricular function is an indication for intervention, imaging should be performed with 2D SSFP or 4DF CMR on a 3 T magnet with ferumoxytol contrast to provide the most accurate data in subjects with concern for low function on echocardiogram. For these reasons, we recommend considering gadobenate dimeglumine-enhanced 4DF obtained on a 1.5-T system as a stand-alone sequence for a comprehensive hemodynamic assessment in patients with rTOF when RV systolic function is clearly normal on a recent echocardiogram. This is particularly attractive in settings in which patients are not able to tolerate a full 2D CMR without sedation but may be able to tolerate a 10-min study.

Limitations of our study include our small study population of pediatric patients with rTOF, which limits the power and generalizability of the findings. Our small study size was in part due to restriction to rTOF patients who received gadobenate, as use of gadofosveset continued at our institution until our supply was depleted, and many were imaged using 3 T and ferumoxytol. The dose of contrast used in this study is above the recommended dose of 0.1 mmol/kg. At the time of this study, it was common practice to administer 1.5–2 × the recommended dose of gadolinium contrast for MR angiography [46]. However, given the growing body of literature demonstrating long-term retention of gadolinium-based contrast agents in tissue (particularly CNS) and the unknown adverse effects thereof [47], the use of contrast

for 4DF CMR is a limitation to its use if an MRA is not already planned. Our practice has since reverted to the recommended dose of 0.1 mmol/kg. While 4DF sequences can be performed without contrast administration, this is not the typical practice at our institution. Prior work on 4DF without contrast have found accurate flow measurements in small cohorts of subjects with congenital heart disease and healthy controls [20, 39], but additional research is necessary prior to consideration of 4DF CMR use without contrast, particularly for volumetry. Although we used 2D CMR as the reference standard for volumetry, 2D SSFP is acquired across a series of breath holds which can vary during the study and thus affect accuracy of the measurements. Therefore, it is possible 4DF may be more accurate as a free breathing acquisition. The temporal resolution chosen in this study is lower than standard practice (~ 20 to 40 ms for 4DF). While this allowed for shorter acquisition times, it likely affected accuracy of our volumetry measurements though we do not believe it dramatically altered flow data based on our experience. Lastly, we did not include localizers in the measurement of 4DF study time which would add on average ~ 60 s per study. While shorter 2D protocols may exist at other institutions allowing for scan times of approximately 45 min, a comprehensive 4DF study would still dramatically reduce scan time.

Future studies with 4DF CMR should continue to understand the clinical utility of 4DF CMR in pediatric CHD with the ultimate goal of demonstrating that 4DF CMR can be performed as a stand-alone sequence in pediatric patients without the use of general anesthesia or intravenous contrast. However, multiple studies are necessary to understand the feasibility and accuracy of 4DF CMR exams in each of these specific contexts. Future studies should utilize valve-tracking techniques and assess peak flow velocity to increase the accuracy of their flow measurements. Further, the accuracy of 4DF CMR should be validated against a gold standard such as clinical outcomes (surgical intervention, remodeling after intervention, symptoms) or invasive methods of measuring volume and flow.

In conclusion, this study demonstrates that in rTOF, 4DF acquisitions may replace 2D PC imaging when gadolinium contrast is already being administered to obtain an MR angiogram. Using a commonly available contrast agent and a 1.5-T system, PNF measured at the PV was more accurate to ANF using 4DF CMR than with 2D CMR. Pulmonary FF was moderately-strongly correlated to RV SV using 4DF and overall similar to 2D CMR. 4DF ventricular volume measurements demonstrated strong correlations and excellent inter-rater reliability, despite a systematic overestimation of volumes compared to 2D CMR. Measurements of EF were only moderately-strongly correlated between methods, as this is a calculated value and propagates error from measured EDV and ESV. A single 4DF acquisition as a stand-alone comprehensive assessment may be considered as an alternative to traditional 2D CMR in standard clinical practice when RV systolic function appears normal by echocardiography, particularly in patients who would require sedation for a standard 2D CMR. We believe that this may represent a major step in optimizing efficiency in pediatric CMR.

Compliance with ethical standards

References

1. Parker SE, Mai CT, Canfield MA, Rickard R, Wang Y, Meyer RE, Anderson P, Mason CA, Collins JS, Kirby RS, Correa A, National Birth Defects Prevention N (2010) Updated National Birth Prevalence estimates for selected birth defects in the United States, 2004–2006. Birth Defects Res A 88(12):1008–1016. https://doi.org/10.1002/bdra.20735

2. Gatzoulis MA, Balaji S, Webber SA, Siu SC, Hokanson JS, Poile C, Rosenthal M, Nakazawa M, Moller JH, Gillette PC, Webb GD, Redington AN (2000) Risk factors for arrhythmia and sudden cardiac death late after repair of tetralogy of Fallot: a multicentre study. Lancet 356(9234):975–981. https://doi.org/10.1016/S0140-6736(00)02714-8

3. Valente AM, Gauvreau K, Assenza GE, Babu-Narayan SV, Schreier J, Gatzoulis MA, Groenink M, Inuzuka R, Kilner PJ, Koyak Z, Landzberg MJ, Mulder B, Powell AJ, Wald R, Geva T (2014) Contemporary predictors of death and sustained ventricular tachycardia in patients with repaired tetralogy of Fallot enrolled in the INDICATOR cohort. Heart 100(3):247–253. https://doi.org/10.1136/heartjnl-2013-304958

4. Knauth AL, Gauvreau K, Powell AJ, Landzberg MJ, Walsh EP, Lock JE, del Nido PJ, Geva T (2008) Ventricular size and function assessed by cardiac MRI predict major adverse clinical outcomes late after tetralogy of Fallot repair. Heart 94(2):211–216. https://doi.org/10.1136/hrt.2006.104745

5. Lee C, Kim YM, Lee CH, Kwak JG, Park CS, Song JY, Shim WS, Choi EY, Lee SY, Baek JS (2012) Outcomes of pulmonary valve replacement in 170 patients with chronic pulmonary regurgitation after relief of right ventricular outflow tract obstruction: implications for optimal timing of pulmonary valve replacement. J Am Coll Cardiol 60(11):1005–1014. https://doi.org/10.1016/j.jacc.2012.03.077

6. Geva T, Gauvreau K, Powell AJ, Cecchin F, Rhodes J, Geva J, del Nido P (2010) Randomized trial of pulmonary valve replacement with and without right ventricular remodeling surgery. Circulation 122(11 Suppl):S201–208. https://doi.org/10.1161/CIRCULATIONAHA.110.951178

7. Bokma JP, Winter MM, Oosterhof T, Vliegen HW, van Dijk AP, Hazekamp MG, Koolbergen DR, Groenink M, Mulder BJ, Bouma BJ (2016) Preoperative thresholds for mid-to-late haemodynamic and clinical outcomes after pulmonary valve replacement in tetralogy of Fallot. Eur Heart J 37(10):829–835. https://doi.org/10.1093/eurheartj/ehv550

8. Oosterhof T, van Straten A, Vliegen HW, Meijboom FJ, van Dijk AP, Spijkerboer AM, Bouma BJ, Zwinderman AH, Hazekamp MG, de Roos A, Mulder BJ (2007) Preoperative thresholds for pulmonary valve replacement in patients with corrected tetralogy of Fallot using cardiovascular magnetic resonance. Circulation 116(5):545–551. https://doi.org/10.1161/CIRCULATIONAHA.106.659664

9. Fratz S, Chung T, Greil GF, Samyn MM, Taylor AM, Valsangiacomo Buechel ER, Yoo SJ, Powell AJ (2013) Guidelines and protocols for cardiovascular magnetic resonance in children and adults with congenital heart disease: SCMR expert consensus group on congenital heart disease. J Cardiovasc Magn Reson 15:51. https://doi.org/10.1186/1532-429X-15-51

10. Valente AM, Cook S, Festa P, Ko HH, Krishnamurthy R, Taylor AM, Warnes CA, Kreutzer J, Geva T (2014) Multimodality imaging guidelines for patients with repaired tetralogy of fallot: a report from the American Society of Echocardiography: developed in collaboration with the Society for Cardiovascular Magnetic Resonance and the Society for Pediatric Radiology. J Am Soc Echocardiogr 27(2):111–141. https://doi.org/10.1016/j.echo.2013.11.009

11. Wald RM, Valente AM, Gauvreau K, Babu-Narayan SV, Assenza GE, Schreier J, Gatzoulis MA, Kilner PJ, Koyak Z, Mulder B, Powell AJ, Geva T (2015) Cardiac magnetic resonance markers of progressive RV dilation and dysfunction after tetralogy of Fallot repair. Heart 101(21):1724–1730. https://doi.org/10.1136/heartjnl-2015-308014

12. Vasanawala SS, Hanneman K, Alley MT, Hsiao A (2015) Congenital heart disease assessment with 4D flow MRI. J Magn Reson Imaging 42(4):870–886. https://doi.org/10.1002/jmri.24856

13. Hsiao A, Alley MT, Massaband P, Herfkens RJ, Chan FP, Vasanawala SS (2011) Improved cardiovascular flow quantification with time-resolved volumetric phase-contrast MRI. Pediatr Radiol 41(6):711–720. https://doi.org/10.1007/s00247-010-1932-z

14. Hsiao A, Lustig M, Alley MT, Murphy M, Chan FP, Herfkens RJ, Vasanawala SS (2012) Rapid pediatric cardiac assessment of flow and ventricular volume with compressed sensing parallel imaging volumetric cine phase-contrast MRI. AJR Am J Roentgenol 198(3):W250–259. https://doi.org/10.2214/AJR.11.6969

15. Hsiao A, Tariq U, Alley MT, Lustig M, Vasanawala SS (2015) Inlet and outlet valve flow and regurgitant volume may be directly and reliably quantified with accelerated, volumetric phase-contrast MRI. J Magn Reson Imaging 41(2):376–385. https://doi.org/10.1002/jmri.24578

16. Hanneman K, Kino A, Cheng JY, Alley MT, Vasanawala SS (2016) Assessment of the precision and reproducibility of ventricular volume, function, and mass measurements with ferumoxytol-enhanced 4D flow MRI. J Magn Reson Imaging 44(2):383–392. https://doi.org/10.1002/jmri.25180

17. van der Hulst AE, Westenberg JJ, Kroft LJ, Bax JJ, Blom NA, de Roos A, Roest AA (2010) Tetralogy of Fallot: 3D Velocity-encoded MR imaging for evaluation of right ventricular valve flow and diastolic function in patients after correction. Radiology 256(3):724–734. https://doi.org/10.1148/radiol.10092269

18. Kamphuis VP, van der Palen RLF, de Koning PJH, Elbaz MSM, van der Geest RJ, de Roos A, Roest AAW, Westenberg JJM (2018) In-scan and scan-rescan assessment of LV in- and outflow volumes by 4D flow MRI versus 2D planimetry. J Magn Reson Imaging 47(2):511–522. https://doi.org/10.1002/jmri.25792

19. Gabbour M, Schnell S, Jarvis K, Robinson JD, Markl M, Rigsby CK (2015) 4-D flow magnetic resonance imaging: blood flow quantification compared to 2-D phase-contrast magnetic resonance imaging and Doppler echocardiography. Pediatr Radiol 45(6):804–813. https://doi.org/10.1007/s00247-014-3246-z

20. Nordmeyer S, Riesenkampff E, Crelier G, Khasheei A, Schnackenburg B, Berger F, Kuehne T (2010) Flow-sensitive four-dimensional cine magnetic resonance imaging for offline blood flow quantification in multiple vessels: a validation study. J Magn Reson Imaging 32(3):677–683. https://doi.org/10.1002/jmri.22280

21. Rahman O, Markl M, Balte P, Berhane H, Blanken C, Suwa K, Dashnaw S, Wieben O, Bluemke DA, Prince MR, Lima J, Michos E, Ambale-Venkatesh B, Hoffman EA, Gomes AS, Watson K, Sun Y, Carr J, Barr RG (2019) Reproducibility and changes in vena caval blood flow by using 4D flow MRI in pulmonary emphysema and chronic obstructive pulmonary disease (COPD): The Multi-Ethnic Study of Atherosclerosis (MESA) COPD Substudy. Radiology 292(3):585–594. https://doi.org/10.1148/radiol.2019182143

22. Geiger J, Markl M, Jung B, Grohmann J, Stiller B, Langer M, Arnold R (2011) 4D-MR flow analysis in patients after repair for tetralogy of Fallot. Eur Radiol 21(8):1651–1657. https://doi.org/10.1007/s00330-011-2108-4

23. Fredriksson A, Trzebiatowska-Krzynska A, Dyverfeldt P, Engvall J, Ebbers T, Carlhall CJ (2018) Turbulent kinetic energy in the right ventricle: potential MR marker for risk stratification of adults with repaired Tetralogy of Fallot. J Magn Reson Imaging 47(4):1043–1053. https://doi.org/10.1002/jmri.25830

24. Sjoberg P, Bidhult S, Bock J, Heiberg E, Arheden H, Gustafsson R, Nozohoor S, Carlsson M (2018) Disturbed left and right ventricular kinetic energy in patients with repaired tetralogy of Fallot: pathophysiological insights using 4D-flow MRI. Eur Radiol 28(10):4066–4076. https://doi.org/10.1007/s00330-018-5385-3

25. Hirtler D, Garcia J, Barker AJ, Geiger J (2016) Assessment of intracardiac flow and vorticity in the right heart of patients after repair of tetralogy of Fallot by flow-sensitive 4D MRI. Eur Radiol 26(10):3598–3607. https://doi.org/10.1007/s00330-015-4186-1

26. Francois CJ, Srinivasan S, Schiebler ML, Reeder SB, Niespodzany E, Landgraf BR, Wieben O, Frydrychowicz A (2012) 4D cardiovascular magnetic resonance velocity mapping of alterations of right heart flow patterns and main pulmonary artery hemodynamics in tetralogy of Fallot. J Cardiovasc Magn Reson 14:16. https://doi.org/10.1186/1532-429X-14-16

27. Cheng JY, Hanneman K, Zhang T, Alley MT, Lai P, Tamir JI, Uecker M, Pauly JM, Lustig M, Vasanawala SS (2016) Comprehensive motion-compensated highly accelerated 4D flow MRI with ferumoxytol enhancement for pediatric congenital heart disease. J Magn Reson Imaging 43(6):1355–1368. https://doi.org/10.1002/jmri.25106

28. Winkelmann S, Schaeffter T, Koehler T, Eggers H, Doessel O (2007) An optimal radial profile order based on the Golden Ratio for time-resolved MRI. IEEE Trans Med Imaging 26(1):68–76. https://doi.org/10.1109/TMI.2006.885337

29. Polte CL, Bech-Hanssen O, Johnsson AA, Gao SA, Lagerstrand KM (2015) Mitral regurgitation quantification by cardiovascular magnetic resonance: a comparison of indirect quantification methods. Int J Cardiovasc Imaging 31(6):1223–1231. https://doi.org/10.1007/s10554-015-0681-3

30. Krieger EV, Lee J, Branch KR, Hamilton-Craig C (2016) Quantitation of mitral regurgitation with cardiac magnetic resonance imaging: a systematic review. Heart 102(23):1864–1870. https://doi.org/10.1136/heartjnl-2015-309054

31. Schulz-Menger J, Bluemke DA, Bremerich J, Flamm SD, Fogel MA, Friedrich MG, Kim RJ, von Knobelsdorff-Brenkenhoff F, Kramer CM, Pennell DJ, Plein S, Nagel E (2013) Standardized image interpretation and post processing in cardiovascular magnetic resonance: Society for Cardiovascular Magnetic Resonance (SCMR) board of trustees task force on standardized post processing. J Cardiovasc Magn Reson 15:35. https://doi.org/10.1186/1532-429X-15-35

32. Feneis JF, Kyubwa E, Atianzar K, Cheng JY, Alley MT, Vasanawala SS, Demaria AN, Hsiao A (2018) 4D flow MRI quantification of mitral and tricuspid regurgitation: reproducibility and consistency relative to conventional MRI. J Magn Reson Imaging 48(4):1147–1158. https://doi.org/10.1002/jmri.26040

33. Zoghbi WA, Adams D, Bonow RO, Enriquez-Sarano M, Foster E, Grayburn PA, Hahn RT, Han Y, Hung J, Lang RM, Little SH, Shah DJ, Shernan S, Thavendiranathan P, Thomas JD, Weissman NJ (2017) Recommendations for noninvasive evaluation of native valvular regurgitation: a report from the American Society of Echocardiography Developed in Collaboration with the Society for Cardiovascular Magnetic Resonance. J Am Soc Echocardiogr 30(4):303–371. https://doi.org/10.1016/j.echo.2017.01.007

34. Haycock GB, Schwartz GJ, Wisotsky DH (1978) Geometric method for measuring body surface area: a height-weight formula validated in infants, children, and adults. J Pediatr 93(1):62–66

35. Bland JM, Altman DG (1986) Statistical methods for assessing agreement between two methods of clinical measurement. Lancet 1(8476):307–310

36. FDA Drug Safety Communication: FDA strengthens warnings and changes prescribing instructions to decrease the risk of serious allergic reactions with anemia drug Feraheme (ferumoxytol).

37. Bailie GR (2012) Comparison of rates of reported adverse events associated with i.v. iron products in the United States. Am J Health Syst Pharm 69(4):310–320. https://doi.org/10.2146/ajhp110262

38. Hanneman K, Sivagnanam M, Nguyen ET, Wald R, Greiser A, Crean AM, Ley S, Wintersperger BJ (2014) Magnetic resonance assessment of pulmonary (QP) to systemic (QS) flows using 4D phase-contrast imaging: pilot study comparison with standard through-plane 2D phase-contrast imaging. Acad Radiol 21(8):1002–1008. https://doi.org/10.1016/j.acra.2014.04.012

39. Nordmeyer S, Riesenkampff E, Messroghli D, Kropf S, Nordmeyer J, Berger F, Kuehne T (2013) Four-dimensional velocity-encoded magnetic resonance imaging improves blood flow quantification in patients with complex accelerated flow. J Magn Reson Imaging 37(1):208–216. https://doi.org/10.1002/jmri.23793

40. O'Brien KR, Cowan BR, Jain M, Stewart RA, Kerr AJ, Young AA (2008) MRI phase contrast velocity and flow errors in turbulent stenotic jets. J Magn Reson Imaging 28(1):210–218. https://doi.org/10.1002/jmri.21395

41. Gatenby JC, McCauley TR, Gore JC (1993) Mechanisms of signal loss in magnetic resonance imaging of stenoses. Med Phys 20(4):1049–1057. https://doi.org/10.1118/1.597001

42. Westenberg JJ, Roes SD, Ajmone Marsan N, Binnendijk NM, Doornbos J, Bax JJ, Reiber JH, de Roos A, van der Geest RJ (2008) Mitral valve and tricuspid valve blood flow: accurate quantification with 3D velocity-encoded MR imaging with retrospective valve tracking. Radiology 249(3):792–800. https://doi.org/10.1148/radiol.2492080146

43. Roes SD, Hammer S, van der Geest RJ, Marsan NA, Bax JJ, Lamb HJ, Reiber JH, de Roos A, Westenberg JJ (2009) Flow assessment through four heart valves simultaneously using 3-dimensional 3-directional velocity-encoded magnetic resonance imaging with retrospective valve tracking in healthy volunteers and patients with valvular regurgitation. Invest Radiol 44(10):669–675. https://doi.org/10.1097/RLI.0b013e3181ae99b5

44. Mooij CF, de Wit CJ, Graham DA, Powell AJ, Geva T (2008) Reproducibility of MRI measurements of right ventricular size and function in patients with normal and dilated ventricles. J Magn Reson Imaging 28(1):67–73. https://doi.org/10.1002/jmri.21407

45. Blalock SE, Banka P, Geva T, Powell AJ, Zhou J, Prakash A (2013) Interstudy variability in cardiac magnetic resonance imaging measurements of ventricular volume, mass, and ejection fraction in repaired tetralogy of Fallot: a prospective observational study. J Magn Reson Imaging 38(4):829–835. https://doi.org/10.1002/jmri.24050

46. Nacif MS, Arai AE, Lima JA, Bluemke DA (2012) Gadolinium-enhanced cardiovascular magnetic resonance: administered dose in relationship to united states food and drug administration (FDA) guidelines. J Cardiovasc Magn Reson 14(1):18. https://doi.org/10.1186/1532-429x-14-18

47. McDonald RJ, Levine D, Weinreb J, Kanal E, Davenport MS, Ellis JH, Jacobs PM, Lenkinski RE, Maravilla KR, Prince MR, Rowley HA, Tweedle MF, Kressel HY (2018) Gadolinium Retention: A Research Roadmap from the 2018 NIH/ACR/RSNA Workshop on Gadolinium Chelates. Radiology 289(2):517–534. https://doi.org/10.1148/radiol.2018181151